Si/Ge exchange mechanisms at the Ge(105) surface

S. Cereda* and F. Montalenti

L-NESS and Dipartimento di Scienza dei Materiali, Università degli Studi di Milano–Bicocca, Via Cozzi 53, I-20125 Milano, Italy

(Received 8 September 2009; revised manuscript received 1 February 2010; published 29 March 2010)

Kinetic pathways for Si adatoms incorporation into Ge(105) are explored by density-functional theory. A very low activation energy (between ~0.6 and ~0.84 eV, depending on strain) for Si/Ge exchanges is found. Consequences on the Ge distribution within SiGe islands on Si(001) are discussed, illustrating why the above processes can influence strain relaxation. Fast exchange processes are shown to take place also in the presence of Si ad-dimers, further facilitating the creation of a Ge floating layer under Si deposition, lowering the surface energy of the exposed facet.

DOI: 10.1103/PhysRevB.81.125439 PACS number(s): 68.43.Bc, 68.47.Fg, 68.35.Fx

I. INTRODUCTION

The Ge(105) surface attracted widespread interest after Mo *et al.*[1] first demonstrated that Ge deposition on Si(001) leads to the formation of hut-shaped nanometric islands bounded by {105} facets. Later studies confirmed the presence of {105} orientations, pointing out that the actual island shape (rectangular huts vs square-based pyramids) depends on the growth conditions, pyramids appearing at higher temperatures.[2] More investigations followed, demonstrating that the Ge(105) surface is indeed an optimal alternative to (001): owed to a peculiar rebonded-step (RS) reconstruction, the (105) surface energy competes with the (001) one, particularly so under the compressive-strain conditions experienced by Ge on Si.[3–9] In order to get more insights into the kinetics of {105} Ge islands growth, also Ge-adatom mobility at such facets was investigated,[10–12] and a step-flow model allowing for fast facet enlargement was proposed.[13]

Nowadays it is well known that, despite the deposition of pure Ge on Si(001), islands tend to be alloyed with temperature-dependent SiGe distributions. Already in 1999, Chaparro *et al.*[14] pointed out that {105} hut clusters grown at $T \geq 550$ °C contained non-negligible amounts of Si. In a further seminal paper the authors showed[15] that Si becomes available when deep enough trenches (drilling the Ge wetting layer and reaching the Si underneath) form around the island perimeter to relieve the strong compression present around the island base.[16,17] In more recent times, SiGe distributions within islands of various shape have been investigated with great detail, exploiting refined x-ray measurements and/or selective etching techniques. Examples can be found in Refs. 18–20, and references therein. Still, from the theoretical point of view, the atomic-scale mechanisms taking place when a Si atom reaches the facets of an island are not completely understood. We are aware only of the recent works presented by Huang *et al.*,[11,12] where hop-diffusion mobility of a Si (and Ge) adatom at the (105) surface is quantified by density-functional theory (DFT) calculations. In this work, instead, we look at possible Si/Ge exchange processes taking place at such surface.

II. METHOD

All results were obtained exploiting DFT calculations using the VASP code[21–23] with ultrasoft pseudopotentials.[24,25] The exchange and correlation term was treated within the Ceperley and Alder local-density approximation (LDA), as parameterized by Perdew and Zunger.[26] The choice of the LDA over the more accurate generalized gradient approximation (GGA) is due to two major reasons. Since the comparison of relaxed and strained systems for a Si adatom on Ge(105) surface is a key point in our calculations, we looked at the Ge and Si mismatch as a key parameter. Being the difference between the experimental equilibrium lattice constant of Si and Ge $\Delta_{exp}=(a_{Ge}-a_{Si})/a_{Ge}=0.04$, and the corresponding values for the LDA and GGA $\Delta_{LDA}=0.04$ and $\Delta_{GGA}=0.05$, respectively, we preferred the LDA due to the better agreement. Moreover this choice allows us to directly compare the results of Refs. 4 and 11–13 where the same exchange and correlation term has been exploited. Nevertheless, we spot checked the effect of gradient corrections by comparing the energy difference between a few minima as computed with LDA and GGA. No significant differences were found. The energy cutoff was set to 240 eV. The simulation slab was composed of 14 (105) layers, and a single (large[4]) unit cell of the (105)RS surface was considered. Calculations were performed both considering the Ge-bulk lattice parameter (corresponding to a 14.422×11.313 Å^2 surface unit cell), and a 4% biaxial compressive strain, representative of Si/Ge lattice mismatch. The latter situation is of particular interest since it mimics the conditions found close to the base of a {105} Ge pyramid on Si(001) (i.e., where Si atoms first arrive[14]), where the in-plane lattice parameter is close to the Si one.[17] Periodic boundary conditions were applied and a vertical vacuum region of ~12 Å was considered. Dangling bonds at the lower slab surface were saturated with hydrogen atoms. The upper surface was instead reconstructed with the typical RS reconstruction. Here we recall that the (105)RS surface is composed of U-shaped structures (Uss) obtained combining three (001) dimers laying on two adjacent (001) terraces.[4] The Brillouin zone was sampled using a $2 \times 3 \times 1$ grid of Monkhorst-Pack points, which turned out to be sufficient to guarantee a good convergence.[13] In geometry optimizations all of the atoms were allowed to relax, except the four bottom layers. Configurational optimizations were achieved by using a conjugate-gradient algorithm. Convergence at local minima (saddle points) was declared when forces were less than 0.005 eV/Å (0.01 eV/Å). In computing activation energies, we used the nudged elastic band method[27] with the climbing-image refinement.[28]

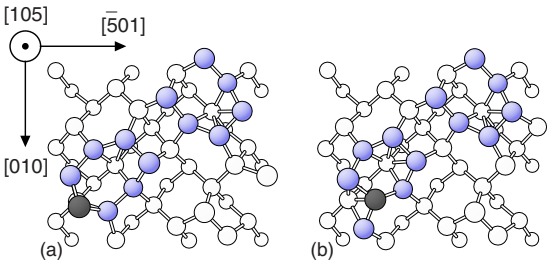

FIG. 1. (Color online) Top view of the Ge(105)RS with an adsorbed adatom (black circle). The Uss of the surface are painted (light blue in the online version). Atoms are represented by circles decreasing in radius with the distance from the surface. (a) Stablest configuration for a Si adatom when a 4% in-plane compressive strain is applied to the surface (this is also the lowest minimum for Ge adatoms on Ge(105)RS, see Ref. 10). (b) Stablest adsorption site for a Si adatom on Ge(105)RS at the equilibrium lattice constant.

III. RESULTS

We initially investigated the dynamical behavior of a Si adatom on the Ge(105)RS with the in-plane lattice parameter set to the Si one. Si hop diffusion for this case was already studied in Ref. 11, where an effective activation barrier E_h $\sim$0.83 eV was reported. Keeping this result in mind, we tried to identify alternative pathways, able to promote Si incorporation into the substrate and the following Ge segregation, i.e., triggering Si/Ge intermixing. At first, we sampled possible binding minima for the isolated Si adatom in order to identify the proper initial configuration, setting the reference energy for estimating the effective activation barriers. To this goal, we started from the Ge/Ge(105)RS adsorption sites presented in Ref. 10, changed the adatom type from Ge to Si, and reoptimized the geometries. The stablest minimum, fully resembling the one already reported for Ge adatoms, is shown in Fig. 1(a). We found several alternative paths leading to Si/Ge intermixing, some with comparable activation energies. In Fig. 2 the lowest-energy one is shown. Starting from the M_1^a site [corresponding to the configuration displayed in Fig. 1(a)], and after a diffusive hop leading to the M_2^a minimum, a two-atom mechanism takes place, leading to configuration M_3^a, where Si is now part of a rather distorted Uss. This is only a metastable situation from which the system quickly evolves, through a set of intermediate configurations (representative local minima M_4^a and M_5^a are reported in Fig. 2) inducing a further shift of the Si atom, until state M_6^a is reached. By comparing M_6^a and M_1^a it is clear that a Ge adatom is now present, while the Si atom is nicely fourfold coordinated, and thus in a stable position. The final configuration M_6^a is $\sim$0.27 eV lower in energy with respect to the initial one M_1^a, reflecting the higher energy of Si dangling bonds with respect to Ge ones. As a consequence, the reverse mechanism bringing back Si to the adatom configuration is less probable. Furthermore, from state M_6^a, the Ge adatom can diffuse along the surface with a lower barrier ($\sim$0.7 eV, see Ref. 10), therefore leaving the Si atom incorporated. The energetics of the path displayed in Fig. 2 is quite complex and requires further investigation to extract at least a semiquantitative estimate of the exchange rate and of

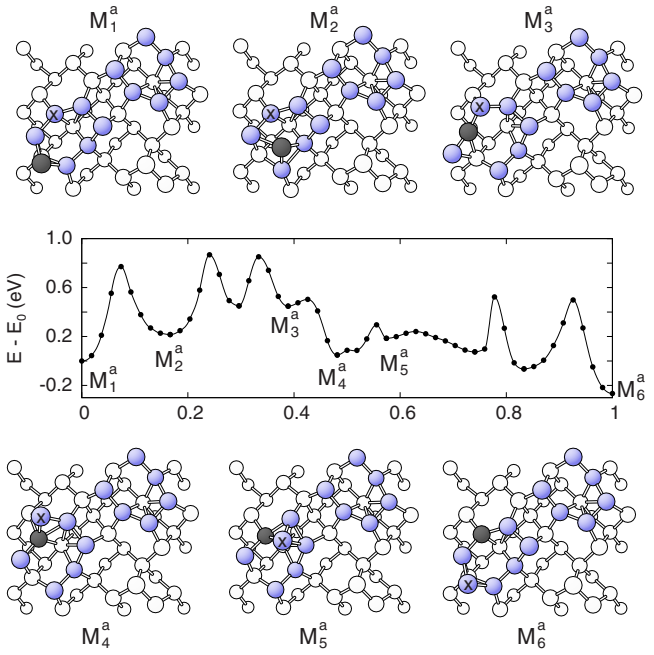

FIG. 2. (Color online) Energy path for a Si adatom (black circle) initially located in its stablest binding site on the Ge(105)RS when an in-plane strain of 4% is applied. E_0 represents the energy of the initial minimum. After an exchange mechanism with one of the Ge atoms composing the Uss (indicated with a cross), the Si adatom is incorporated into the substrate. The energies of the minima and *saddle points* along the path are, from left to right, 0.0 eV (M_1^a), *0.77* eV, 0.22 eV (M_2^a), *0.86* eV, 0.45 eV, *0.85* eV, 0.45 eV (M_3^a), *0.50* eV, 0.05 eV (M_4^a), *0.30* eV, 0.19 eV (M_5^a), *0.24* eV, 0.07 eV, *0.52* eV, −0.06 eV, *0.50* eV, −0.27 eV (M_6^a) (saddle point energies are written in italic).

the relative importance of such mechanism with respect to hop diffusion. From the stablest adsorption site, M_1^a, the Si adatom can attempt either the hop-diffusion process of Ref. 11, or the exchange mechanism of Fig. 2. Since initiating both of them requires surmounting a $\sim$0.8 eV barrier (0.83 eV is the estimate reported in Ref. 11) this will occur with roughly equal probability. Once state M_2^a is reached, the barrier for proceeding along the path is $\sim$0.1 eV higher than the one for aborting the process, therefore returning to the initial site, M_1^a. Similarly, there are other intermediate states along the path where the probability of proceeding toward the final minimum M_6^a or to move in the opposite direction is comparable. If there were no mechanisms competing with the exchange one (imagine in the central panel of Fig. 2 to complete the displayed potential-energy surface by adding a very high barrier $\gg$0.8 eV to be surmounted when attempting to move from M_1^a to the left, i.e., outside the exchange path), the effect of such moves would be to simply lower the effective attempt frequency of the exchange process. This effect can be easily quantified by using simple kinetic Monte Carlo (KMC) simulations (see, e.g., Ref. 10, and the references therein for details) where trajectories are initiated in M_1^a and moves are predicted based on harmonic transition state theory rates, i.e., for each mechanism the rate is estimated using the Arrhenius relation,

$$k = \nu_0 \exp(-E_a/k_B T), \quad (1)$$

where ν_0 is a frequency prefactor set to the standard $\nu_0 = 10^{13}$ s^{-1} value, and E_a the corresponding activation energy inferred from the potential-energy surface of Fig. 2 (see caption for actual values). After averaging over several trajectories, an estimate for the exchange rate k_{ex} is readily obtained as $k_{ex}=1/\langle\tau\rangle$, where $\langle\tau\rangle$ is the average time needed to reach M_6^a from M_1^a. As shown in Fig. 3(a), in the full experimentally relevant temperature range ($T \in [600, 1000]$ K) an Arrhenius relation perfectly describes k_{ex}, with an activation energy $E_{ex}=0.84$ eV and a frequency prefactor $\nu_{ex}=0.3 \times 10^{13}$ s^{-1}. Unsurprisingly, the effective activation energy closely corresponds to the energy difference between the initial minimum and the highest saddle point, while the effective frequency prefactor is lower than the standard one, due to the probability of recrossing barriers which lowers the rate. In order to estimate the relative probability of exchange vs hop diffusion, we must now consider the two processes together. Both start from the same initial minimum, M_1^a. From Ref. 11 one sees that also the hop process is rather complex, involving several metastable states. While the actual hop rate is not calculated in Ref. 11, we can provide an estimate by visual inspection of the reported energetics along the path. The difference between the energy of the initial minimum and the highest saddle point is $E_h=0.83$ eV, i.e., extremely close to our estimate for E_{ex}. Moreover, also the hop path involves visiting states where the probability of aborting the mechanism, returning in the direction of the initial minimum, is higher than the one of proceeding in the desired direction, inducing a reduction in prefactor similar to the one here above reported for the exchange mechanism. We conclude that whenever Si hop diffusion is activated, so it is Si/Ge intermixing, the probability of the two processes being similar.[29]

The above discussed results have important consequences. A Si adatom promoted from the wetting layer to the lower portion of a {105} pyramid will incorporate within the facet before being able to significantly climb toward the top. Only when a sufficient amount of Si occupies subsurface positions, exchanges similar to the one of Fig. 2 can lead to formation of a further Si adatom, allowing for longer effective Si diffusion along the island facets. We find interesting to notice that such delayed Si enrichment toward the top of the island facilitates the reduction in the elastic energy stored in the island. As shown in Refs. 30 and 31, indeed, the lowest-energy state for an island of assigned shape and average Ge concentration is characterized by Si accumulation toward the island base, and Ge segregation at the top. The present calculations show how kinetics helps reaching this situation by exploiting surface processes only.

The results reported in Fig. 2 were obtained under 4% compressive strain conditions. As already recalled, the in-plane lattice parameter becomes closer to the bulk-Ge one toward the apex.[17] It is therefore interesting to check whether strain influences the Si/Ge exchange barrier by repeating the analysis on a fully relaxed Ge(105)RS surface, as a limiting case. Interestingly, the stablest minimum for a Si adatom, reported in Fig. 1(b), changes in the absence of compressive strain. As a consequence, also the minimum-energy path which we found for Si/Ge intermixing is different, as it is clear by comparing Figs. 2 and 4. Notice that at the Ge-bulk lattice parameter the newly formed Ge adatom lays on a different Uss, quite far away from the original Si adatom. The effective activation barrier for this complex multiatom

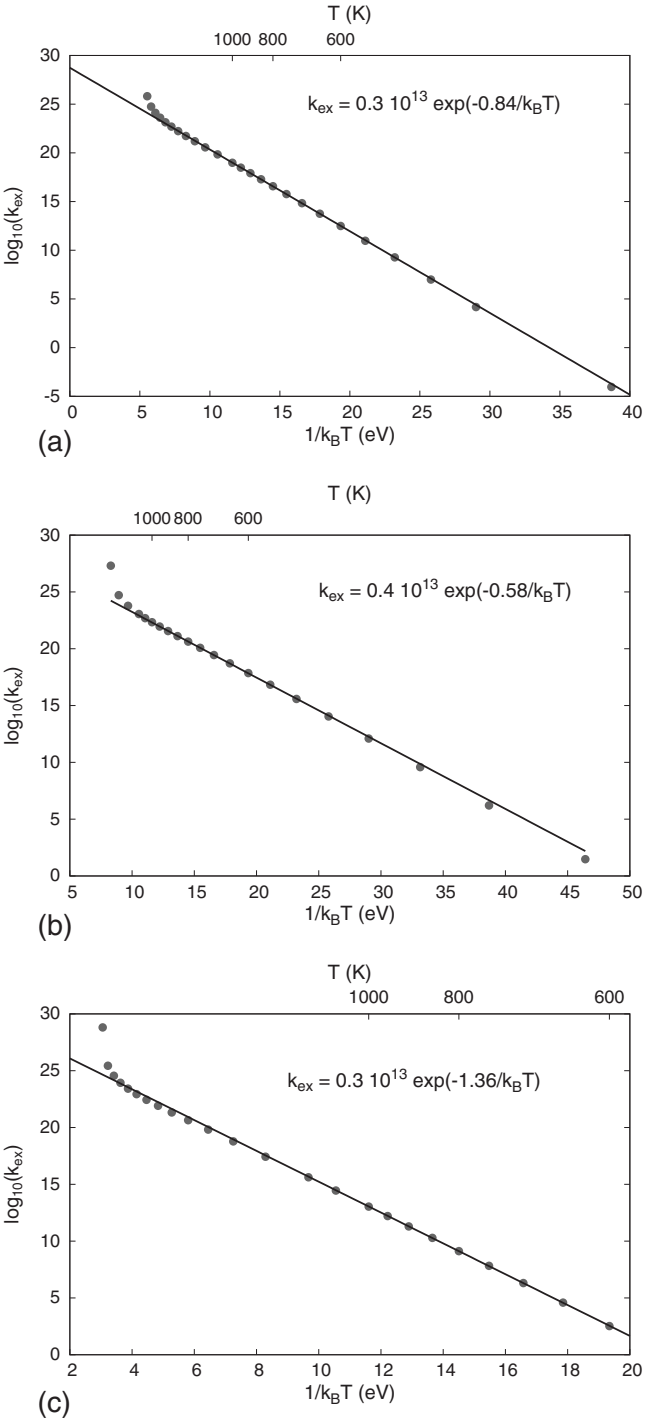

FIG. 3. Effective rates for reaching the final minimum in the investigated mechanisms, as obtained performing KMC simulations at different temperatures. The activation barriers are estimated as best fit in the experimentally relevant range of temperatures 600–1000 K. (a) Effective rate for the path of Fig. 2. (b) Effective rate for the path of Fig. 4. (c) Effective rate for the path of Fig. 5.

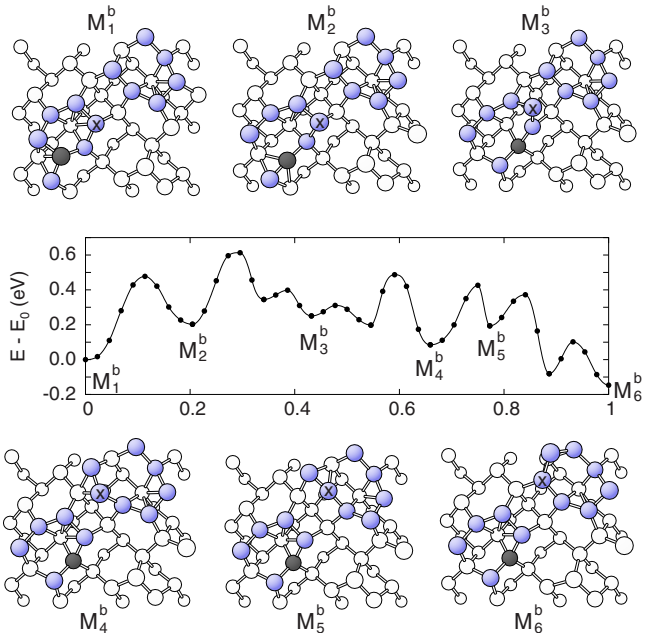

FIG. 4. (Color online) Energy path for a Si adatom (black circle) initially located in its stablest binding site on the Ge(105)RS (configuration M_1^b). E_0 represents the energy of the initial minimum. After an exchange mechanism with one of the Ge atoms composing the Uss (indicated with a cross), the Si adatom is incorporated into the substrate. The segregated Ge atom moves far from its initial position starting up a new exchange mechanism and generating a new Ge adatom. The energies of the relevant points (minima and saddle points) along the path are, from left to right, 0.0 eV (M_1^b), *0.48* eV, 0.20 eV (M_2^b), *0.61* eV, 0.34 eV, *0.40* eV, 0.25 eV (M_3^b), *0.31* eV, 0.20 eV, *0.49* eV, 0.08 eV (M_4^b), *0.43* eV, 0.19 eV (M_5^b), *0.37* eV, −0.08 eV, *0.10* eV, −0.14 eV (M_6^b).

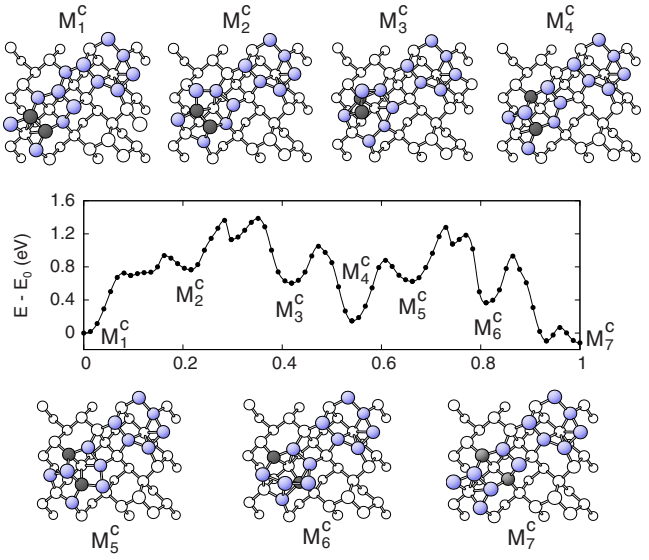

FIG. 5. (Color online) Kinetic path for the complete incorporation of a Si dimer into the substrate. E_0 represents the energy of the initial minimum. Some of the minima along the pathway are shown. The overall activation barrier at the equilibrium lattice parameter (this figure) turns out ~1.36 eV, as obtained from the KMC data shown in Fig. 3(c). In case of a 4% in-plane compression the path is similar but the barrier is slightly lower (~1.2 eV). The energies of the minima and saddle points along the path are, from left to right, 0.0 eV (M_1^c), *0.73* eV, 0.70 eV, *0.94* eV, 0.77 eV (M_2^c), *1.36* eV, 1.13 eV, *1.38* eV, 0.60 eV (M_3^c), *1.05* eV, 0.15 eV (M_4^c), *0.88* eV, 0.62 eV (M_5^c), *1.28* eV, 1.08 eV, *1.18* eV, 0.37 eV (M_6^c), *0.93* eV, −0.09 eV, *0.06* eV, −0.12 eV (M_7^c).

exchange illustrated in Fig. 4 turned out to be even lower [~0.58 vs ~0.84 eV, as obtained from the fitting in the relevant temperatures range shown in Fig. 3(b)] than the corresponding one found under compression: in the most relaxed regions of the island Si incorporation would be (i.e., if Si atoms were able to climb across the facet) faster.

Beside the above discussed influence on the Ge concentration profile within SiGe island, it is worth noticing how the mechanisms of Figs. 2 and 4 clarify how a Ge(105) surface layer is able to float when subject to a Si flux, allowing the system to expose the less energetic surface.[4] This evidence offers a direct atomic-scale justification of dynamic Si/Ge intermixing models treating shallow islands.[32,33] Truly, the isolated adatom case should be always regarded as an ideal one, representative only of the very first stages of Ge covering by Si. It is therefore interesting to check whether, in case a Si-Si ad-dimer is formed, Ge segregation is seriously hindered, therefore freezing the system in a metastable high-energy state. After conducting an extended search for possible paths involving dimers [the starting point being the various configurations reported in Ref. 13 for Ge dimers on Ge(105)RS], we were able to find the mechanism displayed in Fig. 5, noticeably allowing for the complete incorporation of a Si-Si dimer. The initial state represents the stablest configuration for a Si-Si dimer (minimum M_1^c). The mechanism can be considered as a two-step process. In the first part a SiGe dimer (M_4^c) is formed through the exchange of the left Si atom of the dimer. Then a second exchange takes place involving the other tail of the Uss and triggering the segregation of a new GeGe dimer (M_7^c). The above mechanism was found both for unstrained and 4%-compressed Ge(105)RS, the corresponding kinetic barrier being ~1.36 eV in the former case and ~1.2 eV in the latter. As expected, Si-dimer incorporation is slower with respect to the adatom one. Still, by setting the activation energy E_a to the highest 1.36 eV value, and T=773 K (a typical lower limit for Ge/Si growth experiments) and considering as prefactor the one obtained from the fitting of Fig. 3(c), Eq. (1) predicts some 10^3 complete Si-Si dimer incorporation per second. This result shows that even Si ad-dimer formation does not hinder Ge segregation at (105)RS surfaces.

IV. CONCLUSIONS

In this work we have shown that Si/Ge exchanges at the Ge(105)RS facets are fast at typical growth temperatures: whenever hop diffusion is activated, also exchanges are. While any attempt to quantitatively relate our fundamental mechanisms with experiments seems difficult because of the multitude of complex and sometimes unexplored competitive processes taking place (typically, atomic-scale estimates of the actual Si supply through trench formation appears as par-

ticularly difficult to be modeled), several evidences exist supporting fast Si/Ge surface exchanges at {105} facets. Beside the ones already discussed, it is worth recalling the so-called inverse shape transformation, i.e., the observed flattening of island during capping with Si,[34] as a direct consequence of the small lattice mismatch between a strongly alloyed SiGe island and the Si substrate, lowering the need of arranging the atoms in a three-dimensional structure. This phenomenon was directly observed in {105} huts[35–37] and beautifully imaged in the case of dome-shaped islands.[34] In the latter paper, the first portion of the dome islands which was observed to be influenced by capping was the very top where highly relaxed {105} facets are present, i.e., in a region where we predict very fast Si incorporation. On more general grounds, we wish to stress how the present results, and the similar ones obtained on Si(001) (Ref. 38), highlight the importance of complex multiatom exchange mechanisms in Si/Ge systems, where simpler hop diffusion was often considered as the only channel leading to surface mobility.

*Present address: Physics Department, King's College London, Strand, WC2R 2LS London, UK; silvia.cereda@kcl.ac.uk

[1] Y. W. Mo, D. E. Savage, B. S. Swartzentruber, and M. G. Lagally, Phys. Rev. Lett. **65**, 1020 (1990).
[2] G. Medeiros-Ribeiro, A. M. Bratkovski, T. I. Kamins, D. A. A. Ohlberg, and R. S. Williams, Science **279**, 353 (1998).
[3] P. Raiteri, D. B. Migas, L. Miglio, A. Rastelli, and H. von Känel, Phys. Rev. Lett. **88**, 256103 (2002).
[4] D. B. Migas, S. Cereda, F. Montalenti, and L. Miglio, Surf. Sci. **556**, 121 (2004).
[5] Y. Fujikawa, K. Akiyama, T. Nagao, T. Sakurai, M. G. Lagally, T. Hashimoto, Y. Morikawa, and K. Terakura, Phys. Rev. Lett. **88**, 176101 (2002).
[6] T. Hashimoto, Y. Morikawa, Y. Fujikawa, T. Sakurai, M. G. Lagally, and K. Terakura, Surf. Sci. **513**, L445 (2002).
[7] G. H. Lu, M. Cuma, and F. Liu, Phys. Rev. B **72**, 125415 (2005).
[8] G. H. Lu and F. Liu, Phys. Rev. Lett. **94**, 176103 (2005).
[9] O. E. Shklyaev, M. J. Beck, M. Asta, M. J. Miksis, and P. W. Voorhees, Phys. Rev. Lett. **94**, 176102 (2005).
[10] F. Montalenti, D. B. Migas, F. Gamba, and L. Miglio, Phys. Rev. B **70**, 245315 (2004).
[11] L. Huang, G.-H. Lu, F. Liu, and X. Gong, Surf. Sci. **601**, 3067 (2007).
[12] L. Huang, F. Liu, G.-H. Lu, and X. G. Gong, Phys. Rev. Lett. **96**, 016103 (2006).
[13] S. Cereda and F. Montalenti, Phys. Rev. B **75**, 195321 (2007).
[14] S. A. Chaparro, J. Drucker, Y. Zhang, D. Chandrasekhar, M. R. McCartney, and D. J. Smith, Phys. Rev. Lett. **83**, 1199 (1999).
[15] S. Chaparro, Y. Zhang, and J. Drucker, Appl. Phys. Lett. **76**, 3534 (2000).
[16] D. Tambe and V. Shenoy, Appl. Phys. Lett. **85**, 1586 (2004).
[17] G. Vastola, R. Gatti, A. Marzegalli, F. Montalenti, and L. Miglio, in *Self-Assembled Quantum Dots*, edited by Z. Wang (Springer, Berlin, 2008), Chap. 14.
[18] G. Medeiros-Ribeiro and R. Williams, Nano Lett. **7**, 223 (2007).
[19] A. Rastelli, M. Stoffel, A. Malachias, T. Merdzhanova, G. Katsaros, K. Kern, T. Metzger, and O. Schmidt, Nano Lett. **8**, 1404 (2008).
[20] T. Schülli *et al.*, Phys. Rev. Lett. **102**, 025502 (2009).
[21] G. Kresse and J. Hafner, Phys. Rev. B **47**, 558 (1993).
[22] G. Kresse and J. Hafner, Phys. Rev. B **49**, 14251 (1994).
[23] G. Kresse and J. Furthmüller, Phys. Rev. B **54**, 11169 (1996).
[24] D. Vanderbilt, Phys. Rev. B **41**, 7892 (1990).
[25] G. Kresse and J. Hafner, J. Phys.: Condens. Matter **6**, 8245 (1994).
[26] J. P. Perdew and A. Zunger, Phys. Rev. B **23**, 5048 (1981).
[27] H. Jònsson, G. Mills, and K. W. Jacobsen, in *Classical and Quantum Dynamics in Condensed Phase Simulations*, edited by B. J. Berne, G. Ciccotti, and D. F. Coker (World Scientific, Singapore, 1998), p. 383.
[28] G. Henkelman, B. P. Uberuaga, and H. Jónsson, J. Chem. Phys. **113**, 9901 (2000).
[29] A fully quantitative estimate of the exchange vs hop rate is beyond our scopes and would involve a significant extension of the presented calculations. All possible paths, and not simply the minimum-energy ones should be considered, and frequency prefactors ν_0 for all the mechanisms joining adjacent minima along exchange and hop paths should be explicitly computed. This considerable effort is not needed if one is simply willing to shown that hops and exchanges have comparable rates (differences up to a factor $\lesssim 10$ would not change our conclusions).
[30] R. Gatti, F. Uhlík, and F. Montalenti, New J. Phys. **10**, 083039 (2008).
[31] D. Digiuni, R. Gatti, and F. Montalenti, Phys. Rev. B **80**, 155436 (2009).
[32] Y. Tu and J. Tersoff, Phys. Rev. Lett. **93**, 216101 (2004).
[33] Y. Tu and J. Tersoff, Phys. Rev. Lett. **98**, 096103 (2007).
[34] A. Rastelli, M. Kummer, and H. von Känel, Phys. Rev. Lett. **87**, 256101 (2001).
[35] U. Denker, H. Sigg, and O. G. Schmidt, Mater. Sci. Eng., B **101**, 89 (2003).
[36] M. Stoffel, G. S. Kar, U. Denker, A. Rastelli, H. Sigg, and O. G. Schmidt, Physica E **23**, 421 (2004).
[37] U. Denker, H. Sigg, and O. G. Schmidt, Appl. Surf. Sci. **224**, 127 (2004).
[38] F. Zipoli, S. Cereda, M. Ceriotti, M. Bernasconi, L. Miglio, and F. Montalenti, Appl. Phys. Lett. **92**, 191908 (2008).